Dyslipidemia inhibits Toll-like receptor–induced activation of CD8α-negative dendritic cells and protective Th1 type immunity

Abdijapar T. Shamshiev,[1] Franziska Ampenberger,[1] Bettina Ernst,[1] Lucia Rohrer,[2] Benjamin J. Marsland,[1] and Manfred Kopf[1]

[1]Molecular Biomedicine, Institute of Integrative Biology, Swiss Federal Institute of Technology Zürich, 8952 Zürich, Switzerland
[2]Institute of Clinical Chemistry, University Hospital Zürich, 8057 Zürich, Switzerland

Environmental factors, including diet, play a central role in influencing the balance of normal immune homeostasis; however, many of the cellular mechanisms maintaining this balance remain to be elucidated. Using mouse models of genetic and high-fat/cholesterol diet–induced dyslipidemia, we examined the influence of dyslipidemia on T cell and dendritic cell (DC) responses in vivo and in vitro. We show that dyslipidemia inhibited Toll-like receptor (TLR)–induced production of proinflammatory cytokines, including interleukin (IL)-12, IL-6, and tumor necrosis factor-α, as well as up-regulation of costimulatory molecules by CD8α$^-$ DCs, but not by CD8α$^+$ DCs, in vivo. Decreased DC activation profoundly influenced T helper (Th) cell responses, leading to impaired Th1 and enhanced Th2 responses. As a consequence of this immune modulation, host resistance to *Leishmania major* was compromised. We found that oxidized low-density lipoprotein (oxLDL) was the key active component responsible for this effect, as it could directly uncouple TLR-mediated signaling on CD8α$^-$ myeloid DCs and inhibit NF-κB nuclear translocation. These results show that a dyslipidemic microenvironment can directly interfere with DC responses to pathogen-derived signals and skew the development of T cell–mediated immunity.

CORRESPONDENCE
Manfred Kopf:
manfred.kopf@ethz.ch
OR
Abdijapar Shamshiev:
japar.shamshiev@env.ethz.ch

Abbreviations used: APC, allophycocyanin; BMDC, BM-derived DC; DLN, draining LN; HFCD, high-fat/cholesterol diet; HFD, high-fat diet; LDL, low-density lipoprotein; oxLDL, oxidized LDL; nLDL, native LDL; TBARS, thiobarbituric acid–reactive substrates; Tg, transgenic; TLR, Toll-like receptor; VLDL, very LDL.

Immature DCs localize in peripheral tissues, where they are conditioned by environmental factors and act as sentinels against invading pathogens (1). To fulfill their role, DCs constantly sample the microenvironment and capture antigens via receptor-dependent endocytosis, micropinocytosis, and macropinocytosis (2) for subsequent processing and presentation to naive CD4$^+$ T cells. An integral step in this process is the activation of DCs by pathogen-derived structures through pattern-recognition receptors, such as the Toll-like receptor (TLR) family. Upon TLR triggering, DCs up-regulate surface expression of MHC class II, CD40, CD80, and CD86, and release a set of inflammatory cytokines that are critical for full activation of naive CD4$^+$ T cells (3). Depending on the quality of the DC–T-cell interaction, and the constituents of the local cytokine milieu, CD4$^+$ T cells differentiate into distinct subsets called Th1 and Th2. Th1 cells are primarily characterized by their production of IFN-γ and are essential for clearance of intracellular pathogens such as *Leishmania major*, whereas Th2 cells, which produce IL-4, -5, and -13, provide protection from helminth parasites and drive the development of allergies. Th1 cell differentiation is largely driven by the macrophage and DC-derived cytokine IL-12 (4), and, indeed, mice genetically deficient in IL-12 fail to clear *L. major* infection (5, 6). Comparatively, IL-4 is the prototypic inducer of Th2 responses (7, 8); however, instead of DCs, Th2 cells, NKT cells, eosinophils, and basophils are the main sources of IL-4.

Serum, lymph, and interstitial fluid are key components of the environment in which DCs are typically exposed to pathogen-derived structures. Lipoproteins are the main constituents of this extracellular milieu, and perturbation of lipoprotein homeostasis by environmental or genetic factors leads to dyslipidemia. For instance, an excessive consumption of lipid-laden foods and/or a genetic deficiency in the lipid transport

The Journal of Experimental Medicine

protein, apolipoprotein E (apoE), leads to dyslipidemia. Dyslipidemia is a central component of atherosclerosis and metabolic syndromes/pathological conditions linked to chronic inflammation and immune dysfunction (9–11). ApoE-deficient (*apoE*$^{-/-}$) and low-density lipoprotein (LDL) receptor–deficient (*LDLr*$^{-/-}$) mice are commonly used animal models for atherosclerosis and dyslipidemia because when on a standard chow diet they develop spontaneous dyslipidemia, which is characterized by increased plasma levels of very LDL (VLDL), LDL, total cholesterol, and triglycerides (12, 13). These lipoprotein abnormalities become even more severe under a "western-type" diet with a higher cholesterol and fat content (12, 13). Studies using these models have shown that dyslipidemia can alter B cell and CTL responses, and impair host responses against yeast (14), bacterial infections (15, 16), and viral infections (17). In addition, dyslipidemia inhibits migration of skin DCs in *apoE*$^{-/-}$ and *LDLr*$^{-/-}$ mice (18). Thus, dyslipidemia can impair immune responses; however, the underlying mechanisms of its action remain unresolved.

We have examined the influence of dyslipidemia on DC function, on CD4$^+$ Th cell polarization, and on the course of *L. major* infection. Our findings indicate that dyslipidemia directly affects CD8α$^-$ myeloid DCs, impairing their response to TLR stimulation. CD8α$^-$ DCs isolated from dyslipidemic mice exhibited reduced IL-12, -6, and TNF-α production, and they preferentially induced Th2 cell differentiation in vitro. Furthermore, naive CD4$^+$ T cells adoptively transferred into dyslipidemic *apoE*$^{-/-}$ mice differentiated into Th2 cells. This Th2-inducing bias, driven by dyslipidemia, also increased host susceptibility to *L. major* infection, highlighting the considerable impact lipid homeostasis has on host immunity.

RESULTS

Dyslipidemia increases host susceptibility to *L. major* infection

Previous investigations have shown that dyslipidemia can impair antiviral and antibacterial responses (14–17); however, the mechanism has yet to be identified. In particular, it remains unclear whether dyslipidemia leads to an overall immunosuppression or whether it modulates specific immune pathways. Thus, we used an in vivo model of *L. major*

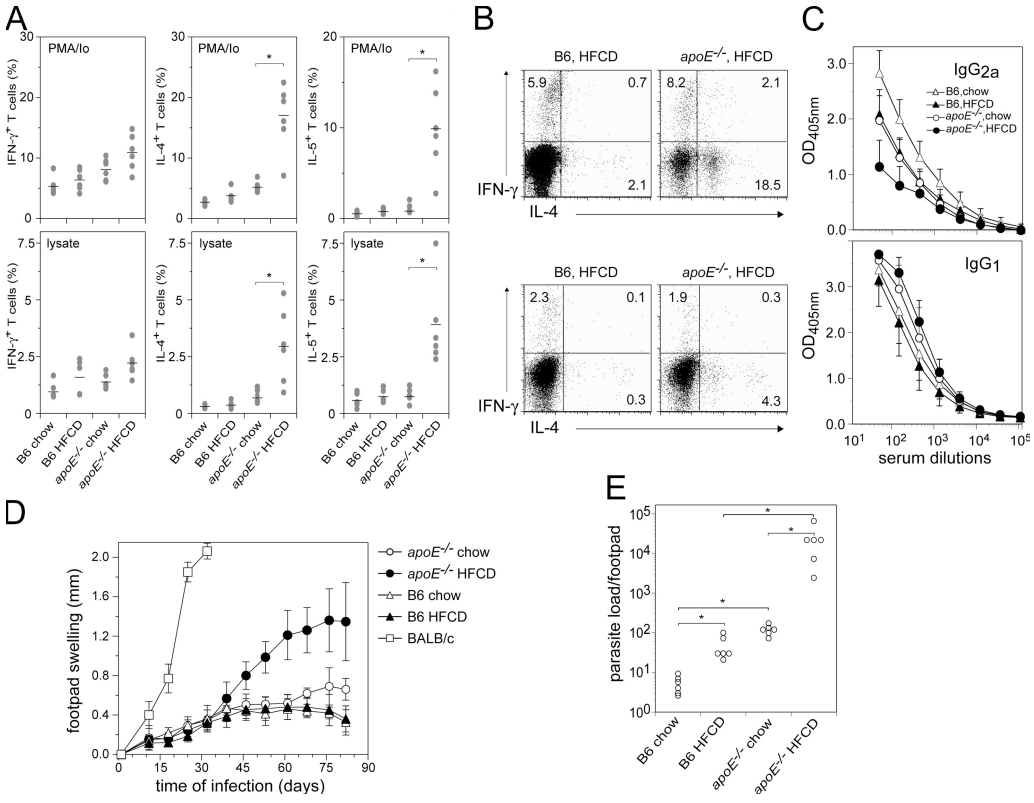

Figure 1. Increased susceptibility to infection with *L. major* in dyslipidemic mice. C57BL/6 (B6) and *apoE*$^{-/-}$ mice were maintained under a chow or HFCD for 8 wk and infected with *L. major*. (A) At 12 wk after infection, DLN cells were restimulated with PMA/ionomycin or *L. major* lysate, and expression of IFN-γ, IL-4, and -5 by CD4$^+$ T cells was determined by flow cytometry. The values show the percentage of IFN-γ, IL-4, and -5 single-positive cells. Horizontal bars indicate mean values for each group. (B) Representative FACS plots of DLN cells from the indicated mice stimulated with either PMA/ionomycin (top) or *L. major* lysate (bottom) are shown. Gated on CD4$^+$ T cells. (C) At 7 wk after infection, serum was collected and *L. major*–specific IgG_{2a} and IgG_1 antibodies were measured by ELISA. Error bars represent the mean ± the SD. (D) Footpad swelling in mice infected with *L. major*. Results are expressed as the mean lesion (millimeters) size ± the SD. (E) Parasite burden in infected mice at 12 wk post-infection. *, $P < 0.05$ compared with indicated controls. Data is representative of similar repeat experiments using 6–10 mice per group.

infection, where the pathways of protective immunity are well established. In particular, C57BL/6 mice develop a Th1 immune response against *L. major* and successfully control the infection, whereas BALB/c mice develop a Th2 response and fail to control the infection (19). *ApoE*$^{-/-}$ and C57BL/6 mice were maintained for 10 wk on either a normal chow diet or a high-fat/cholesterol diet (HFCD) before *L. major* parasites (WHOM/IR/-/173) were injected into the hind footpad. 12 wk after infection, popliteal draining LN (DLN) cells were isolated and restimulated with *L. major* lysate or PMA/ionomycin in vitro. Intracellular cytokine staining revealed that CD4$^+$ T cells from *apoE*$^{-/-}$ mice fed a HFCD exhibited an increase in the number of IL-4– and -5–producing cells compared with C57BL/6 controls (Fig. 1, A and B). In support of these data, *L. major*–specific IgG_{2a} serum titers were reduced in both HFCD-fed *apoE*$^{-/-}$ and C57BL/6 mice compared with chow diet–fed controls (Fig. 1 C), whereas IgG_1 titers were slightly elevated in HFCD-fed *apoE*$^{-/-}$ and C57BL/6 mice as compared with chow diet–fed *apoE*$^{-/-}$ and C57BL/6 animals (Fig. 1 C). These results indicated that the CD4 T-cell response in HFCD-fed *apoE*$^{-/-}$ mice had skewed toward a Th2-type response. In support of this, HFCD-fed *apoE*$^{-/-}$ mice showed increased footpad swelling (Fig. 1 D) and a highly increased parasite burden at the site of infection (Fig. 1 E). Notably, there was also a modest, but significant, increase in swelling and parasite burden in chow diet–fed *apoE*$^{-/-}$ mice compared with chow diet–fed C57BL/6 mice (Fig. 1, D and E). Similar results were obtained using another strain of *L. major* parasites, MHOM/IL/81/FE/BNI (unpublished data). Moreover, wild-type C57BL/6 mice on a long-term (40 wk) high-fat only diet (HFD) showed increased footpad swelling and parasite burden compared with chow diet–fed C57BL/6 mice after *L. major* (WHOM/IR/-/173) infection (unpublished data). Collectively, these data suggest that dyslipidemia promotes Th2 responses and increased susceptibility to *L. major* infection.

ApoE$^{-/-}$ splenic DCs preferentially induce Th2 cell development

Cytokine production and interactions between T cell and DC costimulatory molecules are key mechanisms by which CD4$^+$ T-cell differentiation is driven toward either the Th1 or Th2 subset. We assessed whether dyslipidemia influenced the capacity of DCs to polarize naive CD4$^+$ T cells. Cocultures comprised of splenic DCs and naive CD4TCR transgenic (Tg)

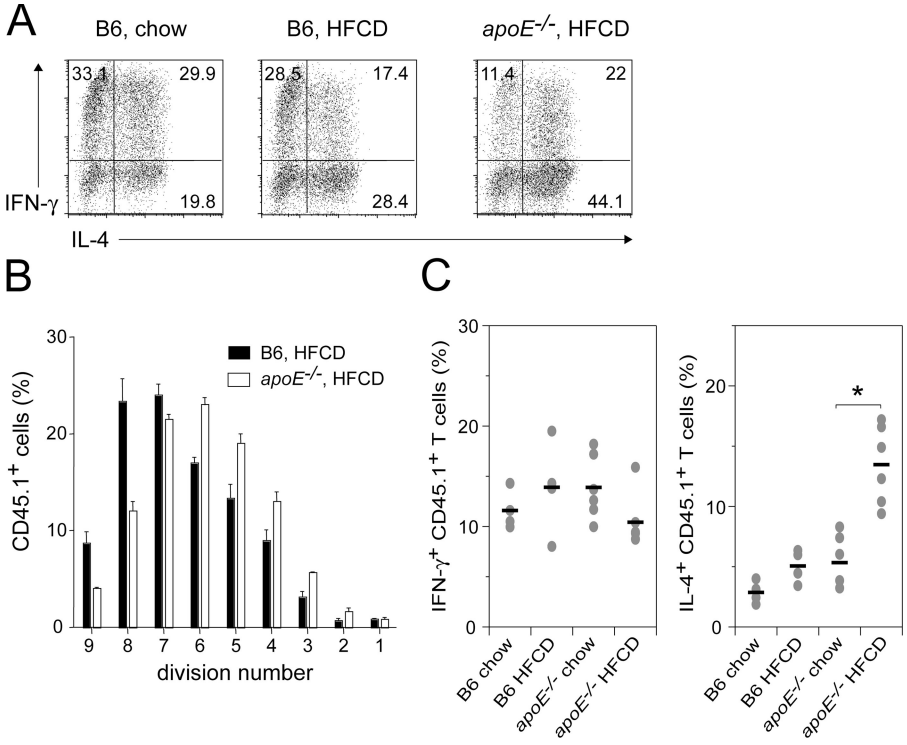

Figure 2. Dyslipidemia promotes Th2 cell development. (A) Splenic DCs were purified from chow diet– or HFCD-fed C57BL/6 (B6) and *apoE*$^{-/-}$ mice, followed by co-culture with naive GP_{61-80}-specific CD4$^+$ T cells in the presence of 10 nM GP_{61-80} peptide. On day 4, the proportion of IL-4– and IFN-γ–producing CD4$^+$ T cells was determined by FACS. Numbers indicate the percentage of cells in each quadrant. (B and C) Naive GP_{61-80}-specific CD4$^+$ T cells (CD45.1$^+$) were CFSE-labeled and transferred i.v. into the indicated mice 1 d before i.p. immunization with 40 μg GP_{61-80} peptide and 5 nmol CpG. (B) After 3 d, CFSE dilution of adoptively transferred cells was determined by FACS. The frequency of cells within each cycle was calculated after appropriate gating on the CFSE$^+$ populations. (C) After 6 d, the production of IFN-γ and IL-4 by adoptively transferred cells was determined by FACS. Horizontal bars indicate mean values for each group (n = 5–6). Error bars represent the mean ± the SD.

T cells specific for a lymphocytic choriomeningitis virus glycoprotein-derived Th cell epitope, GP_{61-80} (20), revealed that DCs isolated from HFCD-fed C57BL/6, and that *apoE*$^{-/-}$ mice preferentially induced IL-4–producing Th2 cells and reduced the frequency of IFN-γ–producing Th1 cells, as compared with DCs isolated from chow diet–fed C57BL/6 controls (Fig. 2 A). Next, we adoptively transferred CFSE-labeled naive CD4$^+$ T cells from congeneic CD45.1$^+$

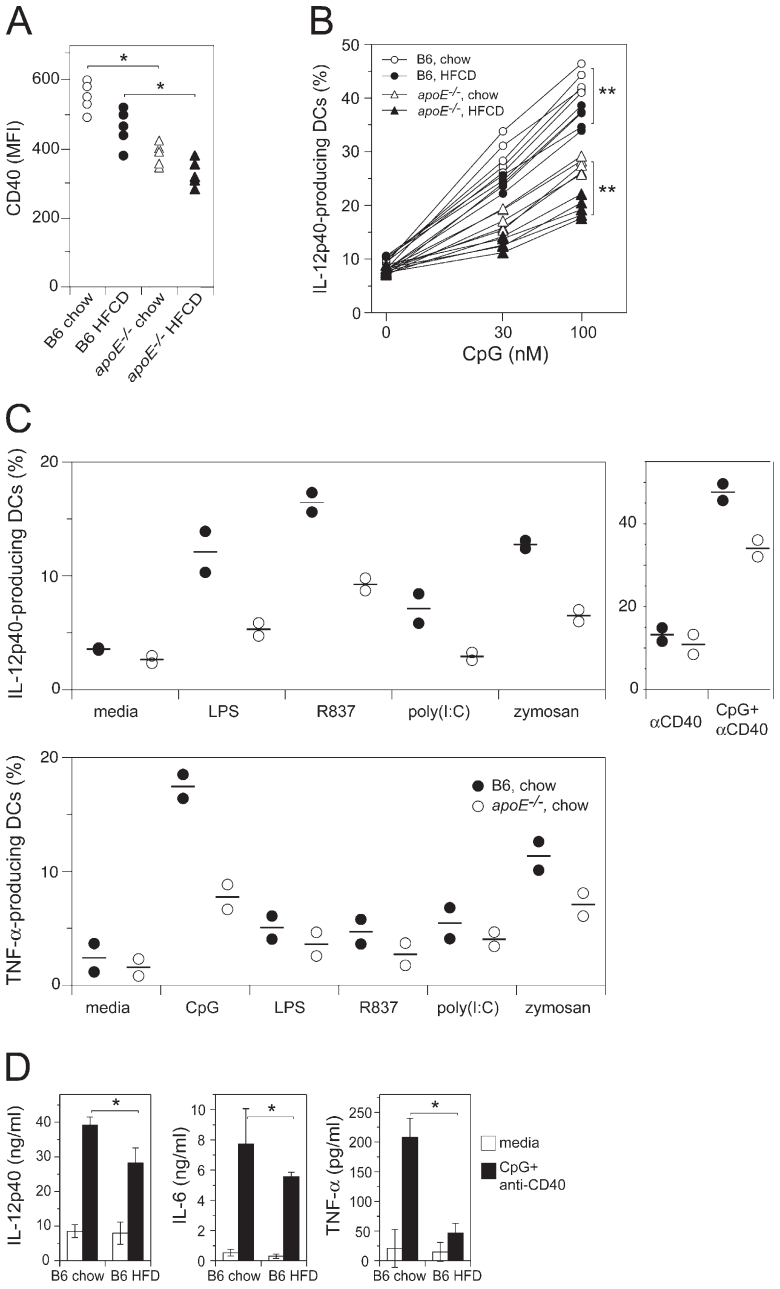

Figure 3. Dyslipidemia inhibits TLR-mediated activation and inflammatory cytokine production of DC. Splenic DCs were isolated from either chow diet– or HFCD-fed C57BL/6 (B6) and *apoE*$^{-/-}$ mice. (A) CD40 surface expression on CD11c$^+$ DCs after stimulation with 100 nM CpG. (B) Isolated cells were stimulated with the indicated doses of CpG for 6 h, followed by surface staining for CD11c and intracellular staining for IL-12p40. (C) Splenic DCs were isolated from chow diet–fed C57BL/6 or *apoE*$^{-/-}$ mice at 30 wk of age and stimulated with 100 nM CpG, 1 μg/ml LPS, 3 μg/ml R837, 5 μg/ml poly(I:C), 30 μg/ml zymosan, 5 μg/ml anti-CD40 antibodies, or a combination of anti-CD40 and CpG (100 nM) for 6 h, followed by surface staining for CD11c and intracellular staining for IL-12p40 and TNF-α. Horizontal bars indicate mean values for each group. (D) Splenic DCs were isolated from C57BL/6 mice fed either chow or HFD for 40 wk and stimulated with CpG/anti-CD40. Supernatants were collected after 20 h of culture and assayed for IL-12p40, IL-6, and TNF-α by ELISA. Data are shown as the mean of values from five mice for each group ± the SD. *, $P < 0.05$; **, $P < 0.01$, compared with indicated controls.

TCR-Tg mice (20) into HFCD-fed CD45.2$^+$ *apoE*$^{-/-}$ or CD45.2$^+$ C57BL/6 mice, and then immunized recipients with $GP_{61\text{-}80}$ peptide together with CpG. After 4 d, at least 8–9 cell divisions were detected in both groups of mice. However, the extent of proliferation was reduced in HFCD-fed *apoE*$^{-/-}$ mice, as compared with chow diet–fed C57BL/6, chow diet–fed *apoE*$^{-/-}$, and HFCD-fed C57BL/6 controls (Fig. 2 B and not depicted), suggesting that CD4 T-cell proliferation was affected by severe dyslipidemia. 6 d after immunization, we restimulated splenocytes with PMA/ionomycin and assessed IL-4 and IFN-γ production by intracellular cytokine staining. The frequency of IFN-γ–producing CD45.1$^+$CD4$^+$ T cells was similar in all four groups of mice, whereas the frequency of IL-4–producing CD45.1$^+$CD4$^+$ T cells was significantly increased in HFCD-fed *apoE*$^{-/-}$ mice compared with *apoE*$^{-/-}$ chow diet, C57BL/6 chow diet, and HFCD controls (Fig. 2 C). These data suggest that dyslipidemia alters the Th1/Th2 balance in vitro and in vivo through a DC-mediated mechanism.

Dyslipidemia impairs TLR-mediated activation of DCs

We next sought to delineate the effect dyslipidemia might have on DC function. *apoE*$^{-/-}$ and C57BL/6 mice were maintained for 12 wk on a standard chow diet or HFCD. The total number of splenic CD11c$^+$ DCs and the expression of costimulatory molecules CD40, CD80, and CD86 under steady-state conditions were similar in all four groups of mice (unpublished data). However, up-regulation of CD40, CD80, and CD86 (Fig. 3 A and not depicted), and the frequency of IL-12p40–producing DCs, were reduced upon CpG stimulation of DCs isolated from mice with genetic dyslipidemia (*apoE*−/−) or diet-induced dyslipidemia (Fig. 3 B). Moreover, DCs from *apoE*$^{-/-}$ mice mounted reduced IL-12p40 and TNF-α responses to stimulation with zymosan, poly(I:C), LPS, and imiquimod (R837), which bind to TLR2, -3, -4, and -7, respectively, as well as to a combination of anti-CD40 mAb and CpG (Fig. 3 C).

To further understand the effects of diet, we assessed DC function in C57BL/6 mice fed with a HFD. After a long-term (35–40 wk) HFD, the production of the proinflammatory cytokines IL-12p40, IL-6, and TNF-α in response to CpG/anti-CD40 stimulation was significantly impaired (Fig. 3 D), whereas DCs were not affected after short-term (6–10 wk) HFD (not depicted). Together, these results demonstrate that both genetic and diet-induced dyslipidemia are associated with impaired maturation and activation of DCs by various TLR ligands.

Impaired DC maturation and cytokine production is restricted to the CD8α$^-$ myeloid subset

Splenic CD11c$^+$ DCs can be classified into CD8α$^-$ (~80% of total) and CD8α$^+$ (~20% of total) subsets that originate from myeloid and lymphoid precursors, respectively (21). Interestingly, impaired IL-12p40 production by *apoE*$^{-/-}$ DCs was only found in the CD8α$^-$, but not in the CD8α$^+$, DC subset (Fig. 4, A and B). DCs require both microbial stimuli and CD40 ligation for optimal production of IL-12p70 (22). Therefore, we stimulated purified CD8α$^-$ and CD8α$^+$ DCs

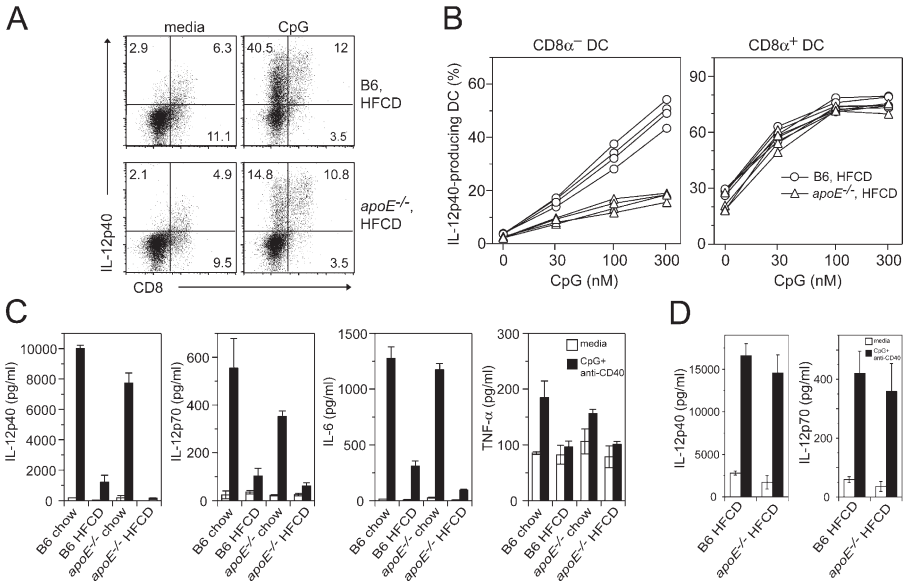

Figure 4. Impaired production of IL-12, -6, and TNF-α in dyslipidemic mice is restricted to the CD8α$^-$ myeloid DC subset. Splenic DCs were isolated from HFCD-fed C57BL/6 (B6) or *apoE*$^{-/-}$ mice and stimulated with CpG for 6 h. (A) Representative dot plots from cells stimulated with 100 nM CpG are shown. (B) The proportion of IL-12p40–producing cells in CD8α$^-$ and CD8α$^+$ DC subsets after stimulation with the indicated doses of CpG. (C) Splenic CD8α$^-$ DCs and (D) CD8α$^+$ DCs were sorted by flow cytometry from C57BL/6 and *apoE*$^{-/-}$ mice were fed either a chow or HFCD for 10 wk and stimulated with CpG and anti-CD40. Supernatants were collected after 20 h of culture and assayed for IL-12p40, -12p35, -6, and TNF-α by ELISA. Error bars represent the mean ± the SD.

with both CpG and agonistic anti-CD40 mAb and measured cytokine production in the supernatant. HFCD strikingly inhibited the capacity of DCs to produce IL-12p40, -12p70, -6, and TNF-α from both C57BL/6 and *apoE*$^{-/-}$ mice with the most severe defect in the latter (Fig. 4 C). In contrast, CD8α^{+} DCs secreted comparable amounts of IL-12p70 and -12p40 (Fig. 4 D). To assess whether dyslipidemia affected the DC response to TLR stimulation in vivo, we injected HFCD-fed *apoE*$^{-/-}$ or C57BL/6 mice with CpG or LPS, and 5 h later we isolated splenic DCs and analyzed expression of costimulatory molecules and IL-12p40 production. Consistent with the in vitro results, we observed a reduced expression of the costimulatory molecules CD80, CD86, and CD40 (Fig. 5 A), and a reduced number of IL-12p40–producing CD8α^{-} DCs isolated from HFCD-fed *apoE*$^{-/-}$ mice (4.6 ± 1.1%) compared with HFCD-fed C57BL/6 controls (15.3 ± 2.4%; Fig. 5 B). Collectively, these results demonstrate that dyslipidemia inhibits TLR-mediated maturation and proinflammatory cytokine production in CD8α^{-} DCs, but not in CD8α^{+} DCs.

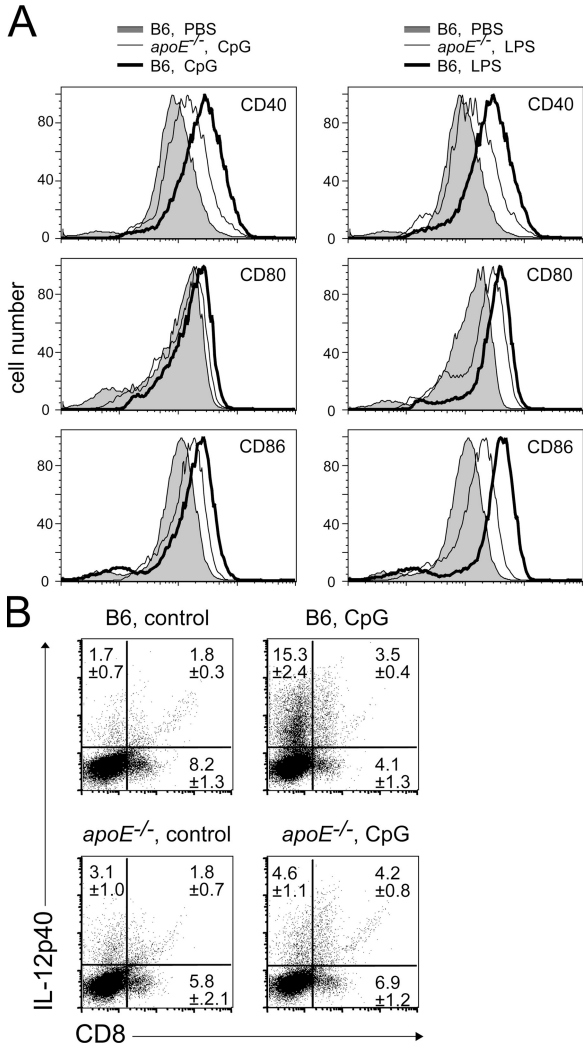

Figure 5. Impaired DC maturation and IL-12 production in dyslipidemic mice after LPS and CpG challenge in vivo. C57BL/6 (B6) and *apoE*$^{-/-}$ mice were fed HFCD for 12 wk, followed by i.v. injection of PBS, 10 nmol CpG, or 30 μg LPS. 5 h after administration, splenic DCs were purified and incubated ex vivo for an additional 12 h. (A) CD11c^{+}CD8α^{-} DCs were analyzed for the expression of CD40, CD80, and CD86 by flow cytometry. The expression levels of CD40, CD80, and CD86 in PBS-injected B6 mice (shaded area) and *apoE*$^{-/-}$ mice (not depicted) were comparable. (B) HFCD-fed C57BL/6 or *apoE*$^{-/-}$ mice were injected i.v. with 10 nmol CpG. 5 h later, splenic DCs were purified and incubated in the presence of Brefeldin A, followed by staining for CD11c, CD8α, and IL-12p40. Numbers indicate the percentage of cells in each quadrant and represent the mean of values from three mice per group. Similar results were obtained with cells isolated from mice injected with LPS.

Dyslipidemia is responsible for the impaired activation of DCs

We next used two strategies to assess whether the impairment of DC maturation and cytokine production was caused by dyslipidemia or simply associated with the absence of *apoE*. First, we generated BM-derived DCs (BMDCs), which are of myeloid origin (23), from chow diet– or HFCD-fed C57BL/6 or *apoE*$^{-/-}$ mice and stimulated them with TLR ligands. All BMDCs responded comparably to LPS, CpG, and poly(I:C), as determined by surface expression of CD40, CD80, CD86, MHC class II, and intracellular staining for IL-12p40, IL-6, and TNF-α (Fig. 6 A and not depicted). Second, we isolated splenic DCs from *apoE*$^{-/-}$ mice at 5 wk of age, i.e., before they had developed severe dyslipidemia. The response of splenic CD8α^{-} DCs isolated from *apoE*$^{-/-}$ mice at 5 wk of age was similar to that of C57BL/6 controls, as shown by intracellular staining for IL-12p40 and surface staining for CD40 and CD80 (Fig. 6 B and not depicted). These results demonstrated that the *apoE*$^{-/-}$ CD8α^{-} DCs were not intrinsically defective because of lack of apoE, and that the impaired response to TLR ligands was likely mediated by dyslipidemia.

Circulating oxidized lipids and oxLDL-induced gene expression in CD8α^{-} DCs are increased in *apoE*$^{-/-}$ mice

Our in vitro data showed that CD8α^{-} DCs from *apoE*$^{-/-}$ mice exhibited impaired responses upon TLR stimulation, and that this phenomenon correlated with dyslipidemia. Dyslipidemia in *apoE*$^{-/-}$ mice is characterized by increased levels of LDL/VLDL, total cholesterol, triglycerides, and altered lipid composition of LDL and high-density lipoprotein (12, 13, 24). In addition, the LDL and VLDL from *apoE*$^{-/-}$ mice are more prone to oxidative modification (25–29). We measured levels of circulating oxidized lipids in 5- or 30-wk-old mice fed a chow diet. At 5 wk of age, C57BL/6 and *apoE*$^{-/-}$ mice exhibited comparable levels of plasma thiobarbituric acid–reactive substrates (TBARS). However, after 30 wk, *apoE*$^{-/-}$ mice presented a statistically significant increase in TBARS (Fig. 7 A). These data are in agreement with previous findings, which show the presence of oxidized lipids in plasma lipoproteins (30, 31) and age-dependent increment of LDL oxidation in *apoE*$^{-/-}$ mice (26, 32). oxLDL has been

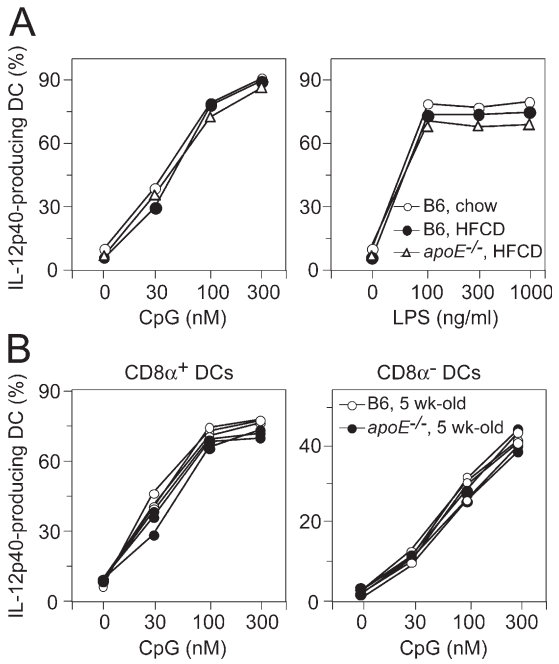

Figure 6. BMDCs generated from HFCD-fed *apoE*$^{-/-}$ mice and splenic DCs from 5-wk-old *apoE*$^{-/-}$ mice exhibit normal responses upon TLR stimulation. (A) C57BL/6 (B6) and *apoE*$^{-/-}$ mice were fed HFCD for 12 wk, and BM cells were pooled from two mice for each group, and BMDCs were generated in GM-CSF–containing media, as described in the Materials and methods. At day 9 of culture, DCs were stimulated with the indicated doses of CpG or LPS for 6 h, followed by surface and intracellular staining. The percentages of CD11c^{+} and IL-12p40^{+} cells for each BMDC culture are shown. Similar results were obtained with poly(I:C)-stimulated cells and intracellular staining for IL-6 and TNF-α. (B) Splenic DCs were purified from C57BL/6 (B6) and *apoE*$^{-/-}$ mice at 5 wk of age and stimulated with CpG for 6 h, followed by surface and intracellular staining. IL-12p40 production was analyzed in CD8α^{+} or CD8α^{-} CD11c^{+} DC subsets. The percentages of IL-12p40^{+} cells for each individual mouse are shown ($n = 3$).

shown to bind the scavenger receptor CD36 (33), leading to increased CD36 expression (34, 35) and levels of adipocyte fatty acid–binding protein (aP2) (36) and ATP-binding cassette A1 (ABCA1) (37). Consistently, we found increased CD36 cell surface expression (Fig. 7 B), as well as ABCA1 and aP2 RNA expression (Fig. 7 C) by CD8α^{-} DCs from *apoE*$^{-/-}$ compared with 30-wk-old C57BL/6 mice. In contrast, CD8α^{+} DCs of C57BL/6 and *apoE*$^{-/-}$ expressed comparable levels of CD36, ABCA1, and aP2 (Fig. 7, B and C). Collectively, these results support the conclusion that oxLDL affects CD8α^{-} DCs in vivo.

oxLDL inhibits NF-κB nuclear translocation in CD8α^{-} DCs and biases their capacity to polarize Th cells

To test whether oxLDL was capable of regulating DC function directly, we pulsed splenic DCs isolated from chow diet–fed C57BL/6 mice with human oxLDL or native LDL (nLDL) before stimulation with CpG or imiquimod (R837). Intracellular cytokine staining revealed that oxLDL treatment inhibited TLR-induced IL-12p40 production in the CD8α^{-} DC subset without affecting the CD8α^{+} DC subset (Fig. 8 A). Consistent with in vitro findings, injection of oxLDL into C57BL/6 mice inhibited IL-12 production by CD8α^{-}, but not CD8α^{+} DCs upon ex vivo CpG stimulation (Fig. 8 B).

In resting cells, NF-κB proteins are primarily localized in the cytoplasm in association with inhibitory proteins. Upon TLR ligation, NF-κB is released from the inhibitory proteins and subsequently translocates into the nucleus to activate proinflammatory gene expression. Consistent with this, we found that upon CpG stimulation of CD8α^{-} BMDCs, NF-κB p65 accumulated in the nucleus, whereas unstimulated cells showed mainly cytoplasmic distribution of NF-κB p65 (Fig. 8 C). In contrast to nLDL, preincubation of DCs with oxLDL prevented CpG-induced translocation of NF-κB p65 into the nucleus (Fig. 8 C), and comparable results were found upon LPS stimulation (not depicted).

We next sought to investigate the effect of oxLDL on Th1/Th2 development in vitro. Thus, DCs were pulsed with oxLDL or nLDL before 4-d co-culture with naive TCR-Tg CD4^{+} T cells and a high concentration of specific antigen (GP_{61-80} peptide), which is a condition favoring Th1 development (38, 39). The Th1-inducing capacity of DCs was considerably impaired upon oxLDL treatment, whereas Th2 development was enhanced (Fig. 8 D).

DISCUSSION

Diseases associated with dyslipidemia are responsible for widespread morbidity and mortality in industrialized countries. The dyslipidemia itself has both direct effects upon disease induction and indirect effects through modulating immune responses. In this study, we have addressed the mechanism by which dyslipidemia effects immune responses in vivo and in vitro. Our data show that CD8α^{-} DCs are conditioned by dyslipidemia to be hyporesponsive, fail to induce robust Th1 responses, and preferentially induce Th2 cell development. Notably, this dyslipidemia-mediated DC hyporesponsiveness had striking implications for protective immunity in vivo.

To facilitate the development of dyslipidemia, we used *apoE*$^{-/-}$ and C57BL/6 mice fed a HFCD. A series of control experiments confirmed that the immune bias in these mice was caused by dyslipidemia, as opposed to other pathways associated with the absence of the *apoE* gene. First, splenic DCs isolated from *apoE*$^{-/-}$ mice at 5 wk of age, i.e., before they develop obvious dyslipidemia and lipid peroxidation, showed normal unimpaired responses to TLR stimulation. The impaired IL-12 production in splenic CD8α^{-} DCs of *apoE*$^{-/-}$ mice was most prominent at 20–30 wk of age, concomitant with the development of severe dyslipidemia and accumulation of lipid peroxidation products. This is consistent with previous studies showing an age- and diet-dependent increase of lipoprotein lipid peroxidation in *apoE*$^{-/-}$ mice (25, 26, 31, 32). Second, HFCD, which accelerates severe dyslipidemia, further impaired DC function in both *apoE*$^{-/-}$ and C57BL/6

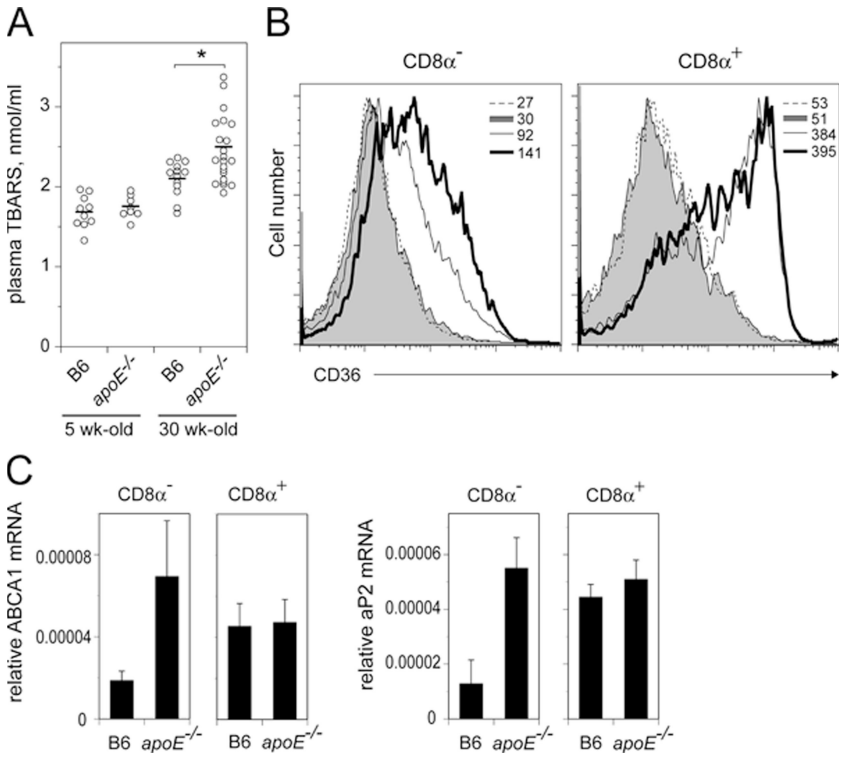

Figure 7. Increased systemic lipid preoxidation and up-regulation of CD36 and oxLDL-induced genes in *apoE*$^{-/-}$ CD8α^{-} DCs. (A) 5- or 30-wk-old, chow diet–fed C57BL/6 mice and *apoE*$^{-/-}$ mice were fasted for 12 h. TBARS were determined in freshly collected plasma samples containing 5 mM EDTA, as described in Materials and methods. (B) CD36 expression was analyzed in splenic DCs isolated from chow diet–fed C57BL/6 (regular line) and *apoE*$^{-/-}$ (bold line) mice at 30 wk of age. Histograms are representative of data obtained from four mice in each group. Mean fluorescence intensity values are shown. Shaded and dashed lines show staining of C57BL/6 and *apoE*$^{-/-}$ DCs with an isotype-matched control antibody, respectively. (C) CD8α^{-} and CD8α^{+} DCs were sorted from the spleens of chow diet–fed C57BL/6 and *apoE*$^{-/-}$ mice at 30 wk of age. ABCA1 and aP2 mRNA levels were quantified by quantitative real time PCR. Horizontal bars indicate mean values for each group (n = 8–22). *, P <0.01, compared with corresponding controls. Error bars represent the mean ± the SD.

mice. Third, BMDCs generated from HFCD-fed *apoE*$^{-/-}$ mice with severe dyslipidemia, in which splenic CD8α^{-} DCs were strongly affected, exhibited unimpaired responses to TLR stimulation. This data also shows that the lack of apoE in the DC, by itself, does not influence DC responses to TLR stimulation. In fact, both HFCD and long-term HFD feeding of C57BL/6 mice reduced TLR-mediated IL-12, -6, and TNF-α production in CD8α^{-} DCs, ruling out a possible DC-intrinsic role for apoE. Thus, we propose that CD8α^{-} DCs are conditioned by the dyslipidemic microenvironment itself, rendering them refractory to stimulation through various TLRs, including TLR2, -3, -4, -7, and -9, which use MyD88- and/or TRIF-dependent signaling pathways to culminate in NF-κB activation (40). We found that oxLDL prevented nuclear translocation of NF-κB p65 in CD8α^{-} DCs. Similarly, oxidized phospholipids that are present in oxLDL have been reported to prevent TLR-induced NF-κB activation in human DC in vitro (41).

Under general conditions, IL-12 plays a central role in the differentiation of naive CD4^{+} T cells into IFN-γ– producing Th1 cells (4), which is further supported by concurrent TLR simulation (42). Our results indicate that dyslipidemia strongly reduces IL-12 production and CD40 up-regulation by splenic CD8α^{-} DCs, in addition to impairing the quality of the TLR signal. Considering that CD40 on DCs is known to positively regulate IL-12 production through its interaction with CD40L on activated T cells (22, 38) this pathway may further compound the immunomodulatory effect of dyslipidemia. In addition to reduced expression of IL-12 and CD40, we found impaired up-regulation of CD80 and CD86, which are critical for optimal activation of CD4^{+} T cells (43, 44). The net result of this impaired expression of costimulatory molecules and reduced production of IL-12 was a bias toward Th2 cell polarization.

A surprising finding was that dyslipidemia influenced the expression of costimulatory molecules and production of inflammatory cytokines exclusively on splenic CD8α^{-} DCs without affecting the CD8α^{+} DC subset. These two DC subsets share a common capacity to present antigens to T cells and induce Th cell differentiation. It has been suggested that CD8α^{+} DCs induce Th1 cell development, whereas CD8α^{-} DCs induce Th2 cell development (45). However, more recent studies showed that the fate of Th cells is greatly influenced by the nature and the concentration of the antigen

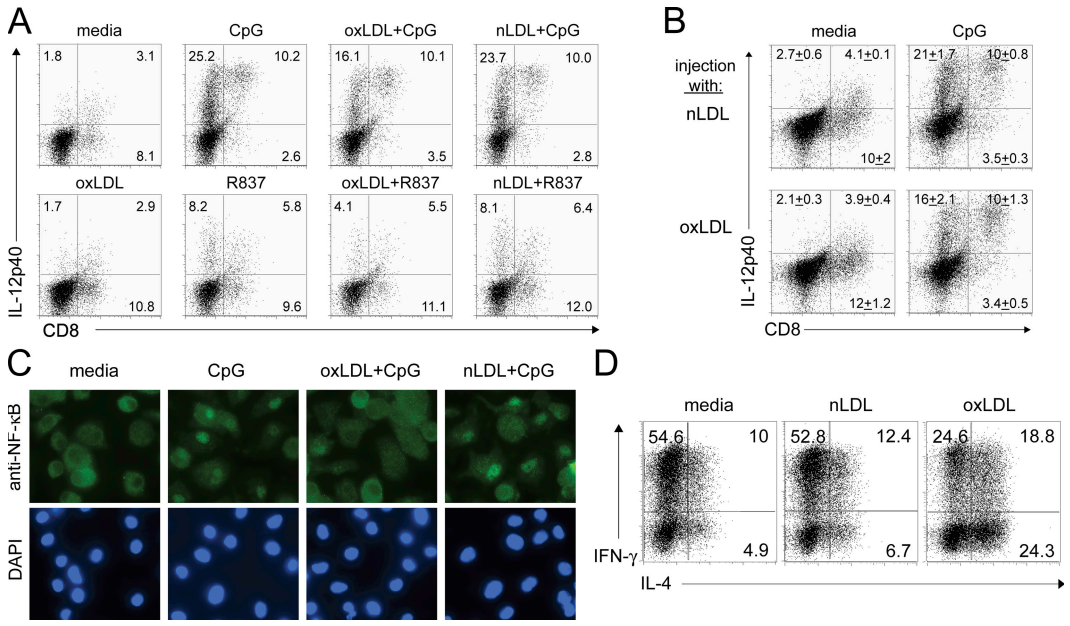

Figure 8. oxLDL inhibits CpG-induced IL-12p40 production and NF-κB nuclear translocation in CD8α⁻ DCs, and promotes Th2 cell differentiation. (A) C57BL/6 splenic DCs were incubated with 40 μg/ml nLDL or 40 μg/ml oxLDL for 1 h at 37°C. After washing, DCs were activated with 100 nM CpG or 5 μg/ml R837 for 6 h, followed by surface staining for CD11c and CD8α, and intracellular staining for IL-12p40. Gated on $CD11c^+$ cells. The numbers indicate the percentage of cells in each quadrant. (B) C57BL/6 mice ($n = 3$) were injected i.v. with 2 mg/dose of either nLDL or oxLDL. After 3 h, splenic DCs were ex vivo stimulated with CpG and stained as described for A. (C) BMDCs were cultured on coverslips and incubated with 60 μg/ml nLDL or 60 μg/ml oxLDL for 1 h, and then stimulated with 300 nM CpG for 30 min at 37°C. Cells were permeabilized and immunostained with anti-NF-κB p65 and Alexa Fluor goat anti-rabbit IgG (green, top); nuclei were stained with DAPI (blue, bottom). (D) C57BL/6 splenic DCs were exposed to10 μg/ml nLDL or 10 μg/ml oxLDL for 1 h and co-cultured with naive GP_{61-80}-specific $CD4^+$ T cells in the presence of 100 nM GP_{61-80} peptide. At day 4, T cells were restimulated with PMA/ionomycin and stained for intracellular IL-4 and IFN-γ. Gated on $CD4^+$ T cells. The numbers indicate the percentage of cells in each quadrant.

(38, 46) and by the activation of DC by microbial stimuli (3, 42, 46). Indeed, both $CD8\alpha^+$ and $CD8\alpha^-$ DCs are capable of inducing either Th1 or Th2 cells, depending on DC stimulating conditions and antigen dose (46, 47).

Our results support previous studies demonstrating that severe hypercholesterolemia reduces IgG_{2a} class switching and enhances KLH-specific IL-4 production (48, 49); Th2-biased autoimmune response to the autoantigen malondialdehyde-LDL (50); and provide a mechanism by which dyslipidemia influences the immune response. Furthermore, using a model of obesity-associated dyslipidemia, our data demonstrates that the effect was not caused by hypercholesterolemia, by itself, but was instead caused by LDL oxidation, and perhaps other disturbances in lipoprotein homeostasis. These data are in agreement with previous studies, which show the antiinflammatory effects of oxLDL in LPS-stimulated macrophages (51–53) and THP-1 cells (54). Still, it remains possible that in addition to oxLDL, reactive oxygen species, including H_2O_2, which is elevated in dyslipidemic conditions (55), may contribute to the impaired DC function in vivo. Additional studies will be required to further define the molecular pathways regulating DC function and Th cell differentiation in dyslipidemia and to identify the downstream lipid metabolites responsible for the inhibitory effect of oxLDL.

Finally, our results have demonstrated that dyslipidemia increases host susceptibility to the intracellular protozoan *L. major,* which is normally controlled by Th1 immune responses. TLR signaling via MyD88-dependent pathways and IL-12 production have been shown to be critical to combat *L. major* infection (5, 6, 56). We have recently described that LN-resident, conduit-associated $CD8\alpha^-$ DCs initiate T-cell responses to *L. major* (57). Thus, reduced activation and IL-12 production by these resident $CD8\alpha^-$ DCs, concomitant with increased frequency of Th2 cytokine-producing cells, is probably responsible for increased susceptibility to *L. major* in dyslipidemic mice. Angeli et al. previously suggested that impaired contact hypersensitivity and delayed-type hypersensitivity are caused by impaired migration of skin DCs in $apoE^{-/-}$ and $LDLr^{-/-}$ mice (18). Consistently, we found that migration of lung and skin DCs to the DLN was reduced in dyslipidemic $apoE^{-/-}$ mice immunized with FITC-coupled ovalbumin (our unpublished data). Thus, although migration of skin DCs is not critical for activation of T cell responses to *L. major* (57), it may contribute to impaired immune responses in other models (18). In fact, impaired DC migration in $apoE^{-/-}$ mice may be a consequence of reduced activation and IL-12p40 (homodimer) production, which has recently been shown to have a potent in vivo chemoattractant activity on DCs (58, 59).

In conclusion, we have shown that dyslipidemia inhibits activation and inflammatory cytokine production by CD8α$^-$ DCs and deviates the ensuing T cell immunity. Our findings have implications for the understanding of the immune mechanisms underlying many pathological conditions in humans, including metabolic syndrome, atherosclerosis, and obesity, which are strongly associated with dyslipidemia.

MATERIALS AND METHODS

Animals. C57BL/6 mice (Charles River Laboratories), *apoE*$^{-/-}$ mice backcrossed to C57BL/6 >10 times (The Jackson Laboratory), and Smarta-2 (a lymphocytic choriomeningitis virus glycoprotein GP_{61-80}) TCR-Tg (I-A^b) mice (20) were maintained in specific pathogen-free conditions. Age-matched (9–12-wk-old) female mice were maintained under either a standard chow diet (3436; Provimi Kliba SA), a HFCD (D12108; Research Diets, Inc.), containing 20% fat and 1.25% cholesterol, or a HFD (2127; Provimi Kliba SA) containing 35% fat and 0.03% cholesterol for the times indicated in the figure legend. All animal experiments were approved and performed under the guidelines set by the State Veterinary Office of Zürich, Switzerland.

Reagents. Human nLDL (RP-031) and oxLDL (RP-047) were obtained from Intracel Resources. LPS from *Escherichia coli* 0111:B4 and zymosan were purchased from Sigma-Aldrich. Phosphorothioate CpG (TCCATGACGTTCCTGATGCT) was synthesized by Microsynth AG. Poly(I:C) and imiquimod (R837) were obtained from InvivoGen.

Isolation of splenic DCs, naive CD4$^+$ T cells, and in vitro differentiation of CD4$^+$ T cells. Splenic CD11c$^+$ DCs were positively sorted from single-cell suspensions of the spleens of C57BL/6 and *apoE*$^{-/-}$ mice, and naive CD4$^+$ T cells were positively sorted from Smarta-2 Tg mice expressing a TCR specific for GP_{61-80} peptide (20) using magnetic beads (Miltenyi Biotec), and in vitro differentiation of naive CD4$^+$ T cells was performed as previously described (42). For some experiments, splenic CD11c$^+$CD8α$^-$ and CD11c$^+$CD8α$^+$ DCs were positively selected from the pooled spleens and sorted using a FACSVantage (97–98% purity; BD Biosciences).

Analysis of cell surface marker expression and detection of intracellular cytokines. FITC-, PE-, or allophycocyanin (APC)-conjugated antibodies specific for CD4, Vα2 TCR, CD62L, CD11c, CD40, I-A^b, CD80, CD86, and CD36 were used for surface staining of CD4$^+$ T cells and DCs. For analysis of DC cytokines, purified DCs were stimulated with the indicated TLR ligands for 2 h and incubated with 10 μg/ml Brefeldin A for an additional 4 h. In some experiments, the combination of CpG and CD40 antibodies was used for DC activation. DCs were surface stained with anti-CD11c and anti-CD8α, fixed in 2% paraformaldehyde for 20 min on ice, permeabilized in 0.5% saponin, and stained intracellularly with anti–IL-12p40-APC, anti–IL-6-PE, or anti–TNF-α–FITC. For analysis of T cell cytokines, CD4$^+$ T cells were stimulated with PMA/ionomycin for 2 h, before the addition of 10 μg/ml Brefeldin A for an additional 2 h. Cells were surface stained with anti-CD4 Abs, fixed, and permeabilized like the DCs, and stained with anti–IFN-γ–APC, anti–IL-4–PE, or anti–IL-5–FITC. Flow cytometry was performed with a FACSCalibur (BD Biosciences) and results were analyzed with FlowJo v6.4.7. (Tree Star, Inc.). All antibodies were obtained from BD Biosciences.

Adoptive transfer and in vivo activation of naive CD4 T cells. Naive CD4$^+$ T cells were labeled with 2.5 μM CFSE (Invitrogen) for 7 min at room temperature and i.v. injected (5×10^6 cells/mouse) into mice 1 d before immunization. At day 0, mice were immunized i.p. with 40 μg GP_{61-80} peptide and 5 nmol CpG DNA mixed in PBS. At day 3, splenocytes were stained for CD45.1, and cell division was analyzed by flow cytometry. To detect cytokines produced by adoptively transferred T cells, mice were killed at day 6, and splenocytes were restimulated with PMA/ionomycin for 2 h, and incubated with 10 μg/ml Brefeldin A for an additional 6 h, followed by surface staining for CD45.1 and intracellular staining for IFN-γ and IL-4.

***L. major* infection and in vitro restimulation of LN cells.** L. major promastigotes WHOM/IR/-/173 (provided by N. Glaichenhaus, Université de Nice-Sophia Antipolis, Valbonne, France), and MHOM/IL/81/FE/BNI (provided by C. Bogdan, University of Freiburg, Freiburg, Germany) were grown as previously described (57). Anesthetized mice were infected in their hind footpad with 2×10^6 metacyclic promastigotes. The size of the footpad lesion was monitored using calipers and presented as the mean value ± the SD from groups of mice ($n \geq 8$). The parasite load was determined using a quantitative limiting-dilution assay. In brief, the footpads and DLN were homogenized and serially diluted in Schneider's medium (Cambrex Bio Science) supplemented with 20% FCS, and then cultured for 7–10 d at 26°C. Parasite burden was expressed as the greatest dilution at which promastigote growth was observed. L. major lysate was prepared by freezing and thawing in PBS, and then being centrifuged at 10,000 g for 10 min at 4°C. The protein concentration in the supernatant containing soluble antigens was determined by the Bradford method using Protein Assay Dye Reagent (Bio-Rad Laboratories). Cell suspensions were prepared from DLN at the indicated times after infection and stimulated with either PMA/ionomycin or L. major lysate for 6 h, followed by fixation and surface staining for CD4 and intracellular staining for IFN-γ, IL-4, and -5.

Real-time quantitative PCR. Total RNA was isolated using TRI Reagent (Molecular Research Center, Inc.) and treated with DNase (Invitrogen) to avoid genomic DNA contamination, followed by reverse transcription using SuperScript III RT (Invitrogen). Quantitative real-time RT-PCR was performed using Brilliant SYBR Green (Stratagene) on an iCycler (Bio-Rad Laboratories). Expression was normalized to β-actin control. Primer sequences are available upon request.

Immunofluorescence analysis. BMDCs were generated as previously described (60) and cultured on coverslips for 3 d. After treatments, cells were fixed in paraformaldehyde (2%) and permeabilized in 0.4% Triton X-100 in PBS. The coverslips were incubated with anti–NF-κB p65 antibodies (sc-7151) in 0.1% Triton X-100 containing 2% goat serum in PBS. Secondary antibodies were Alexa Fluor goat anti–rabbit IgG (Invitrogen). Nuclei were stained with DAPI. The coverslips were mounted on glass slides, and stained cells were examined on a fluorescence microscope (Axioplan 2; Carl Zeiss MicroImaging, Inc.). All cell images were obtained with equal exposure time.

Cytokine detection by ELISA. Culture supernatants were harvested at the indicated times, and TNF-α, IL-6, -12p70, and -12p40 were measured by sandwich ELISA. All antibodies were obtained from eBioscience.

Determination of lipid peroxidation products. Mice were fasted for 12 h before bleeding. The levels of TBARS were determined in freshly collected plasmas by OXItek assay kit (Alexis Corp.) fluorometrically according to manufacturer's instructions.

Statistics. Data are expressed as the mean ± the SD. Statistical comparisons were made using the two-tailed Student's *t* test.

We thank Brian Abel and Alena Donda for critical reading of the manuscript.

This study was supported by Swiss Federal Institute of Technology research grant TH-35/04-2.

The authors have no conflicting financial interests.

Submitted: 14 August 2006
Accepted: 19 January 2007

REFERENCES

1. Kapsenberg, M.L. 2003. Dendritic-cell control of pathogen-driven T-cell polarization. *Nat. Rev. Immunol.* 3:984–993.

2. Sallusto, F., M. Cella, C. Danieli, and A. Lanzavecchia. 1995. Dendritic cells use macropinocytosis and the mannose receptor to concentrate macromolecules in the major histocompatibility complex class II compartment: downregulation by cytokines and bacterial products. *J. Exp. Med.* 182:389–400.
3. Sporri, R., and C. Reis e Sousa. 2005. Inflammatory mediators are insufficient for full dendritic cell activation and promote expansion of CD4+ T cell populations lacking helper function. *Nat. Immunol.* 6:163–170.
4. Hsieh, C.S., S.E. Macatonia, C.S. Tripp, S.F. Wolf, A. O'Garra, and K.M. Murphy. 1993. Development of TH1 CD4+ T cells through IL-12 produced by *Listeria*-induced macrophages. *Science.* 260:547–549.
5. Mattner, F., J. Magram, J. Ferrante, P. Launois, K. Di Padova, R. Behin, M.K. Gately, J.A. Louis, and G. Alber. 1996. Genetically resistant mice lacking interleukin-12 are susceptible to infection with *Leishmania major* and mount a polarized Th2 cell response. *Eur. J. Immunol.* 26:1553–1559.
6. Park, A.Y., B.D. Hondowicz, and P. Scott. 2000. IL-12 is required to maintain a Th1 response during *Leishmania major* infection. *J. Immunol.* 165:896–902.
7. Le Gros, G., S.Z. Ben-Sasson, R. Seder, F.D. Finkelman, and W.E. Paul. 1990. Generation of interleukin 4 (IL-4)-producing cells in vivo and in vitro: IL-2 and IL-4 are required for in vitro generation of IL-4-producing cells. *J. Exp. Med.* 172:921–929.
8. Kopf, M., G. Le Gros, M. Bachmann, M.C. Lamers, H. Bluethmann, and G. Kohler. 1993. Disruption of the murine IL-4 gene blocks Th2 cytokine responses. *Nature.* 362:245–248.
9. Glass, C.K., and J.L. Witztum. 2001. Atherosclerosis. The road ahead. *Cell.* 104:503–516.
10. Hansson, G.K. 2005. Inflammation, atherosclerosis, and coronary artery disease. *N. Engl. J. Med.* 352:1685–1695.
11. Doherty, T.M., E.A. Fisher, and M. Arditi. 2006. TLR signaling and trapped vascular dendritic cells in the development of atherosclerosis. *Trends Immunol.* 27:222–227.
12. Plump, A.S., J.D. Smith, T. Hayek, K. Aalto-Setala, A. Walsh, J.G. Verstuyft, E.M. Rubin, and J.L. Breslow. 1992. Severe hypercholesterolemia and atherosclerosis in apolipoprotein E-deficient mice created by homologous recombination in ES cells. *Cell.* 71:343–353.
13. Zhang, S.H., R.L. Reddick, B. Burkey, and N. Maeda. 1994. Diet-induced atherosclerosis in mice heterozygous and homozygous for apolipoprotein E gene disruption. *J. Clin. Invest.* 94:937–945.
14. Netea, M.G., P.N. Demacker, N. de Bont, O.C. Boerman, A.F. Stalenhoef, J.W. van der Meer, and B.J. Kullberg. 1997. Hyperlipoproteinemia enhances susceptibility to acute disseminated *Candida albicans* infection in low-density-lipoprotein-receptor-deficient mice. *Infect. Immun.* 65:2663–2667.
15. Roselaar, S.E., P.X. Kakkanathu, and A. Daugherty. 1996. Lymphocyte populations in atherosclerotic lesions of apoE −/− and LDL receptor −/− mice. Decreasing density with disease progression. *Arterioscler. Thromb. Vasc. Biol.* 16:1013–1018.
16. de Bont, N., M.G. Netea, P.N. Demacker, I. Verschueren, B.J. Kullberg, K.W. van Dijk, J.W. van der Meer, and A.F. Stalenhoef. 1999. Apolipoprotein E knock-out mice are highly susceptible to endotoxemia and *Klebsiella pneumoniae* infection. *J. Lipid Res.* 40:680–685.
17. Ludewig, B., M. Jaggi, T. Dumrese, K. Brduscha-Riem, B. Odermatt, H. Hengartner, and R.M. Zinkernagel. 2001. Hypercholesterolemia exacerbates virus-induced immunopathologic liver disease via suppression of antiviral cytotoxic T cell responses. *J. Immunol.* 166:3369–3376.
18. Angeli, V., J. Llodra, J.X. Rong, K. Satoh, S. Ishii, T. Shimizu, E.A. Fisher, and G.J. Randolph. 2004. Dyslipidemia associated with atherosclerotic disease systemically alters dendritic cell mobilization. *Immunity.* 21:561–574.
19. Reiner, S.L., and R.M. Locksley. 1995. The regulation of immunity to *Leishmania major*. *Annu. Rev. Immunol.* 13:151–177.
20. Oxenius, A., M.F. Bachmann, R.M. Zinkernagel, and H. Hengartner. 1998. Virus-specific MHC-class II-restricted TCR-transgenic mice: effects on humoral and cellular immune responses after viral infection. *Eur. J. Immunol.* 28:390–400.
21. Shortman, K., and Y.J. Liu. 2002. Mouse and human dendritic cell subtypes. *Nat. Rev. Immunol.* 2:151–161.
22. Schulz, O., A.D. Edwards, M. Schito, J. Aliberti, S. Manickasingham, A. Sher, and C. Reis e Sousa. 2000. CD40 triggering of heterodimeric IL-12 p70 production by dendritic cells in vivo requires a microbial priming signal. *Immunity.* 13:453–462.
23. Wu, L., A. D'Amico, H. Hochrein, M. O'Keeffe, K. Shortman, and K. Lucas. 2001. Development of thymic and splenic dendritic cell populations from different hemopoietic precursors. *Blood.* 98:3376–3382.
24. Zhang, S.H., R.L. Reddick, J.A. Piedrahita, and N. Maeda. 1992. Spontaneous hypercholesterolemia and arterial lesions in mice lacking apolipoprotein E. *Science.* 258:468–471.
25. Hayek, T., J. Oiknine, J.G. Brook, and M. Aviram. 1994. Increased plasma and lipoprotein lipid peroxidation in apo E-deficient mice. *Biochem. Biophys. Res. Commun.* 201:1567–1574.
26. Maor, I., T. Hayek, R. Coleman, and M. Aviram. 1997. Plasma LDL oxidation leads to its aggregation in the atherosclerotic apolipoprotein E-deficient mice. *Arterioscler. Thromb. Vasc. Biol.* 17:2995–3005.
27. Palinski, W., V.A. Ord, A.S. Plump, J.L. Breslow, D. Steinberg, and J.L. Witztum. 1994. ApoE-deficient mice are a model of lipoprotein oxidation in atherogenesis. Demonstration of oxidation-specific epitopes in lesions and high titers of autoantibodies to malondialdehyde-lysine in serum. *Arterioscler. Thromb.* 14:605–616.
28. Palinski, W., S. Horkko, E. Miller, U.P. Steinbrecher, H.C. Powell, L.K. Curtiss, and J.L. Witztum. 1996. Cloning of monoclonal autoantibodies to epitopes of oxidized lipoproteins from apolipoprotein E-deficient mice. Demonstration of epitopes of oxidized low density lipoprotein in human plasma. *J. Clin. Invest.* 98:800–814.
29. Neuzil, J., J.K. Christison, E. Iheanacho, J.C. Fragonas, V. Zammit, N.H. Hunt, and R. Stocker. 1998. Radical-induced lipoprotein and plasma lipid oxidation in normal and apolipoprotein E gene knockout (apoE−/−) mice: apoE−/− mouse as a model for testing the role of tocopherol-mediated peroxidation in atherogenesis. *J. Lipid Res.* 39:354–368.
30. Shih, D.M., Y.R. Xia, X.P. Wang, E. Miller, L.W. Castellani, G. Subbanagounder, H. Cheroutre, K.F. Faull, J.A. Berliner, J.L. Witztum, and A.J. Lusis. 2000. Combined serum paraoxonase knockout/apolipoprotein E knockout mice exhibit increased lipoprotein oxidation and atherosclerosis. *J. Biol. Chem.* 275:17527–17535.
31. Forte, T.M., G. Subbanagounder, J.A. Berliner, P.J. Blanche, A.O. Clermont, Z. Jia, M.N. Oda, R.M. Krauss, and J.K. Bielicki. 2002. Altered activities of anti-atherogenic enzymes LCAT, paraoxonase, and platelet-activating factor acetylhydrolase in atherosclerosis-susceptible mice. *J. Lipid Res.* 43:477–485.
32. Aviram, M., M. Rosenblat, C.L. Bisgaier, R.S. Newton, S.L. Primo-Parmo, and B.N. La Du. 1998. Paraoxonase inhibits high-density lipoprotein oxidation and preserves its functions. A possible peroxidative role for paraoxonase. *J. Clin. Invest.* 101:1581–1590.
33. Endemann, G., L.W. Stanton, K.S. Madden, C.M. Bryant, R.T. White, and A.A. Protter. 1993. CD36 is a receptor for oxidized low density lipoprotein. *J. Biol. Chem.* 268:11811–11816.
34. Nagy, L., P. Tontonoz, J.G. Alvarez, H. Chen, and R.M. Evans. 1998. Oxidized LDL regulates macrophage gene expression through ligand activation of PPARgamma. *Cell.* 93:229–240.
35. Tontonoz, P., L. Nagy, J.G. Alvarez, V.A. Thomazy, and R.M. Evans. 1998. PPARgamma promotes monocyte/macrophage differentiation and uptake of oxidized LDL. *Cell.* 93:241–252.
36. Fu, Y., N. Luo, and M.F. Lopes-Virella. 2000. Oxidized LDL induces the expression of ALBP/aP2 mRNA and protein in human THP-1 macrophages. *J. Lipid Res.* 41:2017–2023.
37. Venkateswaran, A., B.A. Laffitte, S.B. Joseph, P.A. Mak, D.C. Wilpitz, P.A. Edwards, and P. Tontonoz. 2000. Control of cellular cholesterol efflux by the nuclear oxysterol receptor LXR alpha. *Proc. Natl. Acad. Sci. USA.* 97:12097–12102.
38. Ruedl, C., M.F. Bachmann, and M. Kopf. 2000. The antigen dose determines T helper subset development by regulation of CD40 ligand. *Eur. J. Immunol.* 30:2056–2064.
39. Marsland, B.J., T.J. Soos, G. Spath, D.R. Littman, and M. Kopf. 2004. Protein kinase C θ is critical for the development of in vivo T helper (Th)2 cell but not Th1 cell responses. *J. Exp. Med.* 200:181–189.
40. Akira, S., and K. Takeda. 2004. Toll-like receptor signalling. *Nat. Rev. Immunol.* 4:499–511.

41. Bluml, S., S. Kirchberger, V.N. Bochkov, G. Kronke, K. Stuhlmeier, O. Majdic, G.J. Zlabinger, W. Knapp, B.R. Binder, J. Stockl, and N. Leitinger. 2005. Oxidized phospholipids negatively regulate dendritic cell maturation induced by TLRs and CD40. *J. Immunol.* 175:501–508.
42. Nembrini, C., B. Abel, M. Kopf, and B.J. Marsland. 2006. Strong TCR signaling, TLR ligands, and cytokine redundancies ensure robust development of type 1 effector T cells. *J. Immunol.* 176:7180–7188.
43. Lumsden, J.M., J.M. Roberts, N.L. Harris, R.J. Peach, and F. Ronchese. 2000. Differential requirement for CD80 and CD80/CD86-dependent costimulation in the lung immune response to an influenza virus infection. *J. Immunol.* 164:79–85.
44. Harris, N.L., M. Prout, R.J. Peach, B. Fazekas de St Groth, and F. Ronchese. 2001. CD80 costimulation is required for Th2 cell cytokine production but not for antigen-specific accumulation and migration into the lung. *J. Immunol.* 166:4908–4914.
45. Maldonado-Lopez, R., T. De Smedt, P. Michel, J. Godfroid, B. Pajak, C. Heirman, K. Thielemans, O. Leo, J. Urbain, and M. Moser. 1999. CD8α+ and CD8α$^-$ subclasses of dendritic cells direct the development of distinct T helper cells in vivo. *J. Exp. Med.* 189:587–592.
46. Boonstra, A., C. Asselin-Paturel, M. Gilliet, C. Crain, G. Trinchieri, Y.J. Liu, and A. O'Garra. 2003. Flexibility of mouse classical and plasmacytoid-derived dendritic cells in directing T helper type 1 and 2 cell development: dependency on antigen dose and differential Toll-like receptor ligation. *J. Exp. Med.* 197:101–109.
47. Manickasingham, S.P., A.D. Edwards, O. Schulz, and C. Reis e Sousa. 2003. The ability of murine dendritic cell subsets to direct T helper cell differentiation is dependent on microbial signals. *Eur. J. Immunol.* 33:101–107.
48. Zhou, X., G. Paulsson, S. Stemme, and G.K. Hansson. 1998. Hypercholesterolemia is associated with a T helper (Th) 1/Th2 switch of the autoimmune response in atherosclerotic apo E-knockout mice. *J. Clin. Invest.* 101:1717–1725.
49. Robertson, A.K., X. Zhou, B. Strandvik, and G.K. Hansson. 2004. Severe hypercholesterolaemia leads to strong Th2 responses to an exogenous antigen. *Scand. J. Immunol.* 59:285–293.
50. Binder, C.J., K. Hartvigsen, M.K. Chang, M. Miller, D. Broide, W. Palinski, L.K. Curtiss, M. Corr, and J.L. Witztum. 2004. IL-5 links adaptive and natural immunity specific for epitopes of oxidized LDL and protects from atherosclerosis. *J. Clin. Invest.* 114:427–437.
51. Ohlsson, B.G., M.C. Englund, A.L. Karlsson, E. Knutsen, C. Erixon, H. Skribeck, Y. Liu, G. Bondjers, and O. Wiklund. 1996. Oxidized low density lipoprotein inhibits lipopolysaccharide-induced binding of nuclear factor-kappaB to DNA and the subsequent expression of tumor necrosis factor-alpha and interleukin-1beta in macrophages. *J. Clin. Invest.* 98:78–89.
52. Chung, S.W., B.Y. Kang, S.H. Kim, Y.K. Pak, D. Cho, G. Trinchieri, and T.S. Kim. 2000. Oxidized low density lipoprotein inhibits interleukin-12 production in lipopolysaccharide-activated mouse macrophages via direct interactions between peroxisome proliferator-activated receptor-gamma and nuclear factor-kappa B. *J. Biol. Chem.* 275:32681–32687.
53. Hourton, D., D. Stengel, M.J. Chapman, and E. Ninio. 2001. Oxidized low density lipoproteins downregulate LPS-induced platelet-activating factor receptor expression in human monocyte-derived macrophages: implications for LPS-induced nuclear factor-kappaB binding activity. *Eur. J. Biochem.* 268:4489–4496.
54. Mikita, T., G. Porter, R.M. Lawn, and D. Shiffman. 2001. Oxidized low density lipoprotein exposure alters the transcriptional response of macrophages to inflammatory stimulus. *J. Biol. Chem.* 276:45729–45739.
55. Furukawa, S., T. Fujita, M. Shimabukuro, M. Iwaki, Y. Yamada, Y. Nakajima, O. Nakayama, M. Makishima, M. Matsuda, and I. Shimomura. 2004. Increased oxidative stress in obesity and its impact on metabolic syndrome. *J. Clin. Invest.* 114:1752–1761.
56. de Veer, M.J., J.M. Curtis, T.M. Baldwin, J.A. DiDonato, A. Sexton, M.J. McConville, E. Handman, and L. Schofield. 2003. MyD88 is essential for clearance of *Leishmania major*: possible role for lipophosphoglycan and Toll-like receptor 2 signaling. *Eur. J. Immunol.* 33:2822–2831.
57. Iezzi, G., A. Frohlich, B. Ernst, F. Ampenberger, S. Saeland, N. Glaichenhaus, and M. Kopf. 2006. Lymph node resident rather than skin-derived dendritic cells initiate specific T cell responses after *Leishmania major* infection. *J. Immunol.* 177:1250–1256.
58. Khader, S.A., S. Partida-Sanchez, G. Bell, D.M. Jelley-Gibbs, S. Swain, J.E. Pearl, N. Ghilardi, F.J. Desauvage, F.E. Lund, and A.M. Cooper. 2006. Interleukin 12p40 is required for dendritic cell migration and T cell priming after *Mycobacterium tuberculosis* infection. *J. Exp. Med.* 203:1805–1815.
59. Reinhardt, R.L., S. Hong, S.J. Kang, Z.E. Wang, and R.M. Locksley. 2006. Visualization of IL-12/23p40 in vivo reveals immunostimulatory dendritic cell migrants that promote Th1 differentiation. *J. Immunol.* 177:1618–1627.
60. Lutz, M.B., R.M. Suri, M. Niimi, A.L. Ogilvie, N.A. Kukutsch, S. Rossner, G. Schuler, and J.M. Austyn. 2000. Immature dendritic cells generated with low doses of GM-CSF in the absence of IL-4 are maturation resistant and prolong allograft survival in vivo. *Eur. J. Immunol.* 30:1813–1822.